

STRUCTURAL AND OPTICAL PROPERTIES OF ZnO NANOSTRUCTURES

Swee-Yong Pung¹, Kwang-Leong Choy², and Xianghui Hou²

¹ School of Materials and Mineral Resources Engineering, Universiti Sains Malaysia, Pulau Pinang, Malaysia, Tel: +60-604 5995215, e-mail: sypung@eng.usm.my

² Faculty of Engineering, Energy and Sustainability Research Division, Department of Mechanical, Materials and Manufacturing Engineering, University Park, University of Nottingham, United Kingdom

Received Date: November 29, 2011

Abstract

The structural and crystal quality of ZnO film, Au-catalyzed ZnO nanowires (NWs) and catalyst-free ZnO NWs were studied. ZnO film deposited at 145°C by atomic layer deposition (ALD) had a smooth surface (RMS roughness: 2.850 nm), high transmittance in the visible light region (89.9±6.7%) and good film resistivity (4.131x10⁻³ Ω.cm). Thus, ZnO films with these attractive properties are suitable for transparent conducting oxide (TCO) applications. Both catalyst-free ZnO NWs and Au-catalyzed ZnO NWs were grown using chemical vapour deposition (CVD). Vertically aligned ZnO NWs (catalyst-free) could be synthesized using highly (002) oriented ZnO seed film pre-deposited on silicon substrate. The catalyst-free ZnO NWs exhibited the best crystal quality as it showed the largest percentage of Zn-O bonds in XPS analysis and highest UV/visible ratio in PL measurement. However, randomly grown Au-catalyzed ZnO NWs were synthesized on bare silicon substrate. The randomly grown NWs has been attributed to the large lattice mismatch between ZnO and silicon wafer. The growth of Au-catalyzed ZnO NWs was proposed to be governed by Vapour-Liquid-Solid_Vapour-Solid (VLS-VS) mechanism.

Keywords: Atomic layer deposition, Chemical vapour deposition, Nanowires, Thin films, ZnO

Introduction

ZnO is an attractive compound semiconductor with a wide band gap ($E_g = 3.3$ eV) and a large exciton binding energy (~ 60 meV) at room temperature. It is one of a few materials that are suitable for fabrication of optoelectronic devices in short wave region [1] attributes to these unique properties. Furthermore, ZnO can be used for various applications such as field effect transistor [2], solar cells [3] and surface acoustic wave devices [4].

Various techniques have been used to grow ZnO thin film and nanostructures. For examples, Radio Frequency (RF) sputtering [5], Pulsed Laser Deposition (PLD) [6] and Metal Organic Chemical Vapour Deposition (MOCVD) [7] have been used to deposit ZnO film. On the other hand, Chemical Vapour Deposition (CVD) [8] and direct oxidation from Zn metal block [9] have been used to grow ZnO NWs. In order to realize the importance of using ZnO nanostructures in the above mentioned applications, it is necessary to produce ZnO nanostructures with good crystal quality at relatively low synthesis temperature.

In this work, the structural and optical properties of ZnO film, catalyst-free ZnO NWs and Au-catalyzed ZnO NWs were studied. The ZnO film was deposited using atomic layer deposition at 145°C, whereas ZnO NWs were grown using chemical vapour deposition at 650°C.

Experimental Method

Atomic layer deposition (ALD, Cambridge Nanotech, Savannah 100) was used to deposit ZnO thin films on Si substrates (p-type, (100)) and glasses. Diethylzinc (DEZn) and water (H₂O) were used as precursors for deposition of ZnO thin films. The ALD chamber was evacuated by a rotary pump (50 to 70 Pa) before the manual valve of the DEZn bubbler was turned on. The vapors of both precursors were purged alternately into the chamber through separate inlet lines. The deposition temperature was set at 145°C. The details of the deposition procedure and conditions were reported elsewhere [8].

Highly (002) ZnO seed film and 5 nm thick Au film were pre-deposited on silicon substrates using ALD (280°C, 1200 cycles) and sputtering, respectively. The growth of ZnO NWs was carried out in a horizontal tube reactor at 2 kPa and 650°C. Zn powder (99.99% purity) was loaded in the middle of quartz tube of the reactor. The substrates were loaded at the downstream of the reactor. The reactor was heated to 650°C under a constant flow of argon gas (95 sccm). After reaching the desired temperature, oxygen gas (5 sccm) was flowed into the furnace for 30 minutes for the growth of NWs.

The crystalline structure of ZnO nanostructures were characterized by transmission electron microscope (TEM, JEOL, JEM-2100F). The surface morphology of the nanostructures was examined using a scanning electron microscope (SEM, Philips XL30 ESEM-FEG). X-ray photoelectron microscope (VG Scientific, ESCALAB Mark II, Al_{Kα} radiation with wavelength of 1486.6 eV) was used to characterize the chemical bonds of these specimens. The measurement area of each samples was 1mm x 1mm. Photoluminescence (PL) studies were performed on these ZnO specimens with N₂ laser excitation source (337 nm, pulse rate 20 Hz). The surface roughness of ZnO thin films was measured by atomic force microscope (AFM, Veeco CPII-Research Scanning Probe Microscope) in contact mode. The sheet resistance (R_s) of ZnO thin films was determined using the Van der Pauw resistivity measurement technique. The optical transmittance spectra were measured by a Biochrom Libra S22 UV/Vis spectrometer in the wavelength range of 300 - 850 nm. The thickness of ZnO layer was measured using ellipsometer (Jobin Yvon, MM16).

Results and Discussion

ZnO Film

Figure 1 shows the morphology of thin film deposited at 145°C (1200 process cycles, 0.015s DEZn and 0.015s H₂O). It consists of a number of tiny and longish grains. The RMS surface roughness of the film measured by AFM in contact mode was found to be 2.850 nm. The stoichiometry of this film was characterized by XPS. As shown in Figure 2, the presence of the Zn LMN Auger peak at 498.0 eV and the O 1s peak at 530.4eV verifies that the as-deposited film was ZnO. The ratio of atomic percentage of Zn to O was 56.5%: 43.5%. The thickness of ZnO film was 232.1±10.4 nm as measured by ellipsometer.

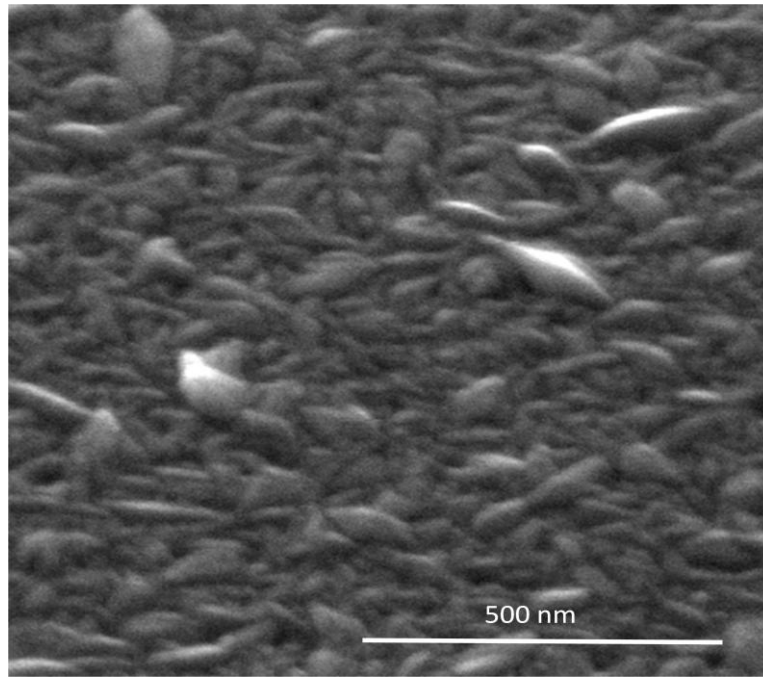


Figure 1. SEM image of thin film deposited at 145°C (1200 process cycles, 0.015s DEZn and 0.015s H₂O)

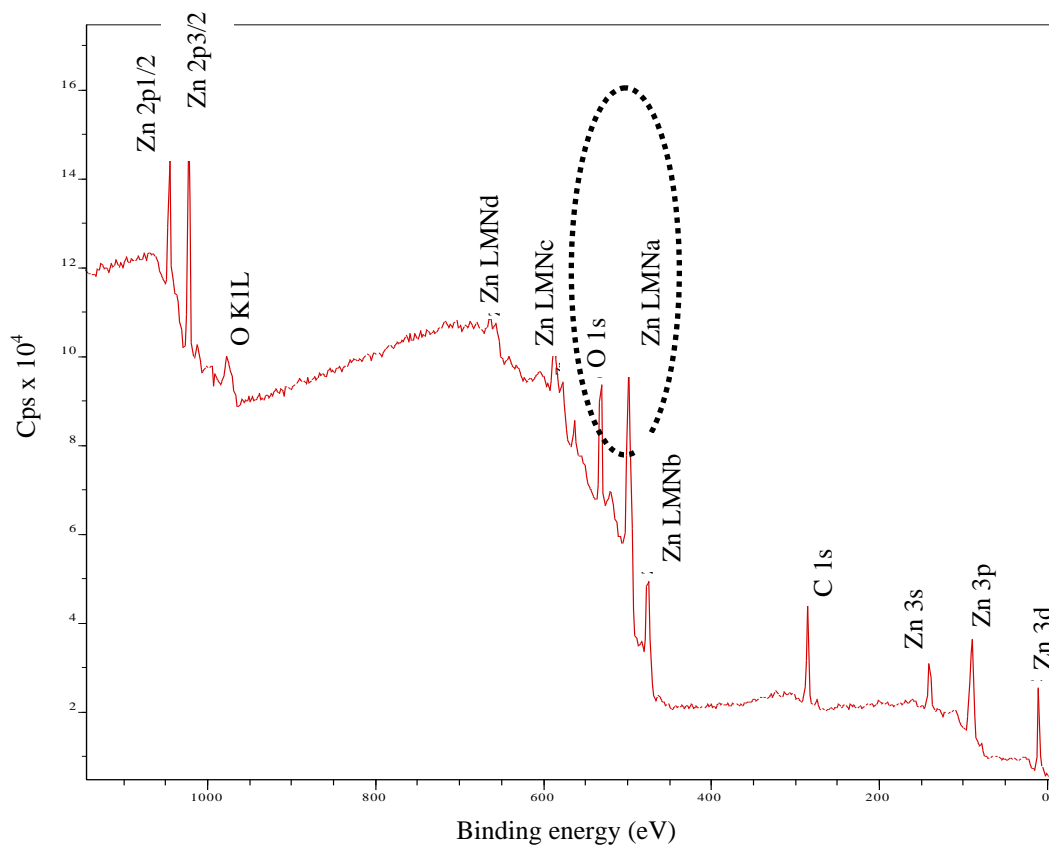


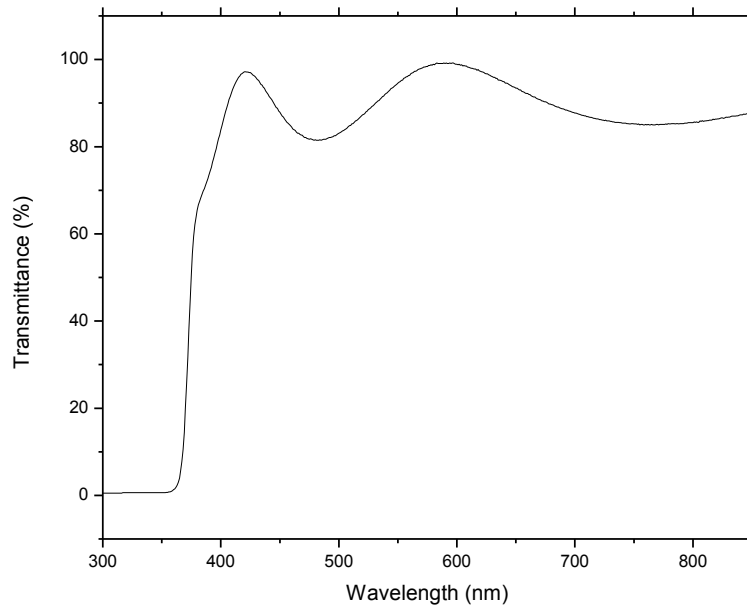
Figure 2. XPS spectrum of the film deposited at 145°C (1200 process cycles, 0.015s DEZn and 0.015s H₂O)

The ZnO film coated on glass substrate was highly transparent under visible light. As displayed in Figure 3 (a), the transmittance of this ZnO film in the visible light region (380 to 750 nm) was 89.9 ± 6.7 %. It exhibits a sharp ultraviolet cut-off at approximately 365 nm. The energy gap (E_g) was estimated by assuming a direct transition between valence and conduction bands using equation (1):

$$\alpha h\nu = K(h\nu - E_g)^{1/2} \quad (1)$$

where K is a constant, E_g is determined by extrapolating the straight line portion of the spectrum to $\alpha h\nu = 0$. From Figure 3 (b), the optical energy gap (E_g) of 3.26 eV is deduced. This value is slightly smaller than the bulk value ($E_g = 3.31$ eV) [10]. However, it is in good agreement with reported value of ZnO thin films [11-12].

(a)



(b)

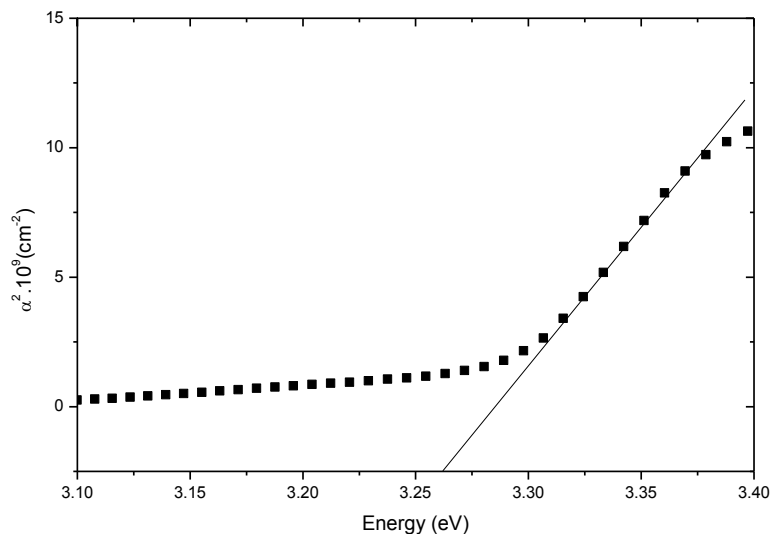


Figure 3. (a) UV-Vis spectrum and (b) plot of α^2 vs photon energy ($h\nu$) of ZnO film deposited at 145 C (1200 process cycles, 0.015s DEZn and 0.015s H₂O)

Furthermore, the film resistivity measured by the Van der Pauw technique showed promising results (e.g. $4.131 \times 10^{-3} \Omega \cdot \text{cm}$). Therefore, it could be concluded that highly transparent ZnO film had been successfully grown by the ALD technique using DEZn and H_2O as precursors.

Catalyst-Free ZnO NWs

Catalyst-free ZnO NWs were grown on ZnO seed film pre-deposited on silicon surface using CVD. In this study, highly (002) oriented ZnO seed film was needed to facilitate the aligned growth of catalyst-free ZnO NWs [8] as shown in Figure 4 (a) and 4 (b). The average diameter, length and aspect ratio of catalyst-free ZnO NWs was $87.78 \pm 22.19 \text{ nm}$, $256.67 \pm 28.76 \text{ nm}$ and 3.10 ± 0.81 , respectively. Figure 4 (c) shows the HRTEM image of the ZnO NWs. This image reveals a clear lattice spacing of 0.52 nm corresponding to the interplanar spacing of wurtzite ZnO (002) which indicates that the growth of the ZnO NWs occurred preferentially along the [0001] direction. The SAED analysis of the ZnO NWs confirmed that the NW was single-crystalline in structure as seen in Figure 4 (d). It is worth mentioning that synthesis condition that allows moderate growth rate is also required to produce aligned NWs with uniform diameter [13].

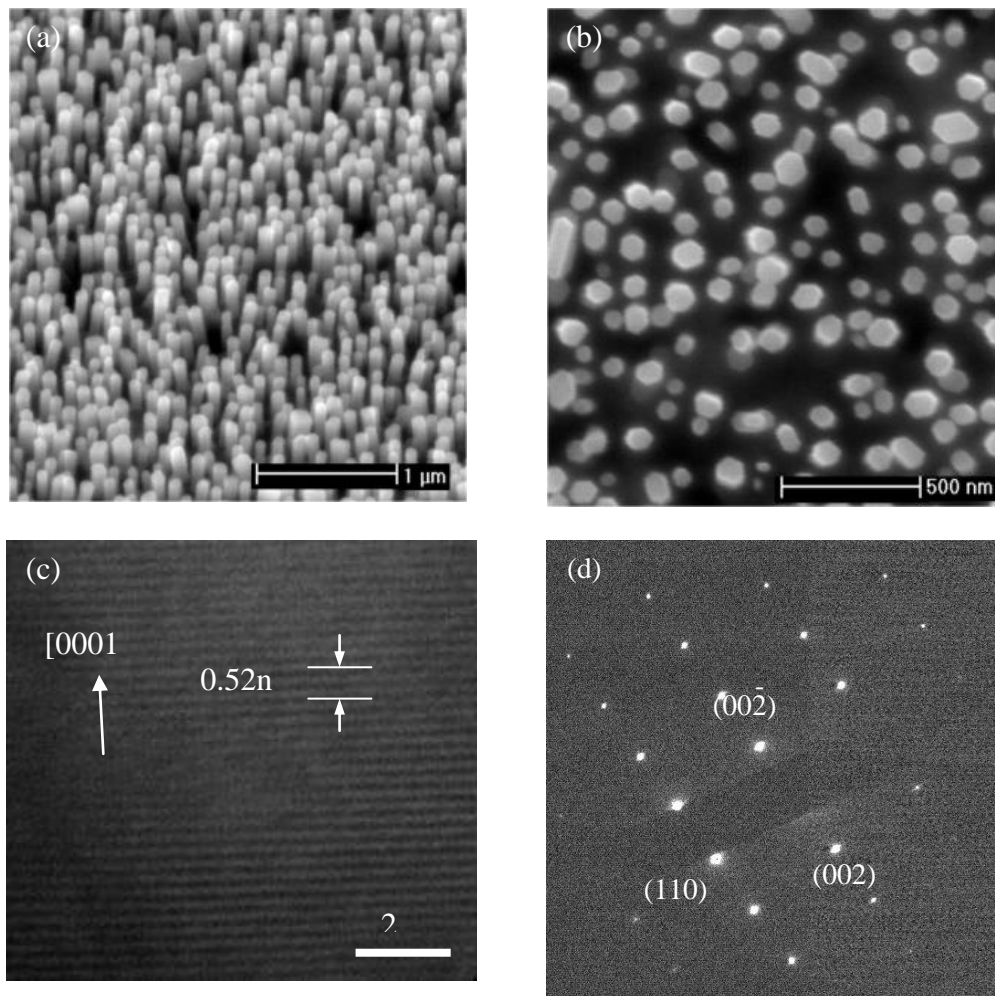


Figure 4. Catalyst-free ZnO NWs grown by CVD, (a) side view (SEM), and (b) top view (SEM), (c) HRTEM and (d) SAED

The growth of catalyst-free ZnO NWs was governed by Vapor-Solid (VS) mechanism. The surface energy of a plane, which can be related to the effectiveness of capturing the adsorbed atoms, decides the growth rate and the proportion of crystallographic planes such as {001}, {100} and {101} in the final structure under certain supersaturation level of Zn and O vapours. In the case of ZnO, the (002) plane has the lowest surface free energy, followed by the {100} planes. Thus, ZnO NWs have the highest growth rate in [0001] direction, followed by the $\langle 10\bar{1}0 \rangle$. Generally, low supersaturation of Zn and O vapours is favoured for the growth of perfect crystals, i.e. a well-faceted hexagonal ZnO NWs.

Au-catalyzed ZnO NWs

As shown in Figure 5, randomly grown Au-catalyzed ZnO NWs was synthesized on silicon substrate attributed to the large lattice mismatch between ZnO and Si [14]. The average diameter, length and aspect ratio of Au-catalyzed ZnO NWs was 63.12 ± 21.63 nm, 344.15 ± 82.73 nm and 6.45 ± 3.51 , respectively. Au alloy nanoparticles (highlighted in circles) could be found at the base and at the tip of the NWs.

Generally, the growth of Au-catalyzed ZnO NWs was suggested to govern by VLS mechanism [15]. In VLS mechanism, Au-Si liquid droplets served as preferential sites for absorption of the gas phase of the Zn and oxygen reactants. When the liquid droplets were supersaturated with the reactants, they became the nucleation sites for ZnO crystallization. The solid-liquid interface formed the growth interface. It acted as a sink causing the continued Zn and O incorporation into the lattice and, thereby, the growth of the ZnO NW with the alloy droplet riding on the top. Since the (001) plane has the highest atomic packing density, NWs tend to grow in the [0001] direction in order to achieve minimum surface free energy. The growth of NWs continued as long as the catalyst alloy remains in a liquid state and the reactant is available.

However, we propose that two possible growth mechanisms, i.e. VLS and VS mechanism, could possibly occur at the same time during the growth of Au-catalyzed ZnO NWs. VLS mechanism occurred at the Au alloy droplets (nanoparticles) while VS mechanism occurred at the side facets of NWs. The growth of ZnO NWs continued as long as the supply of Zn and O vapor was available. Therefore, it is more appropriate to describe that the growth of Au-catalyzed ZnO NWs was governed by the combined VLS-VS mechanism [16].

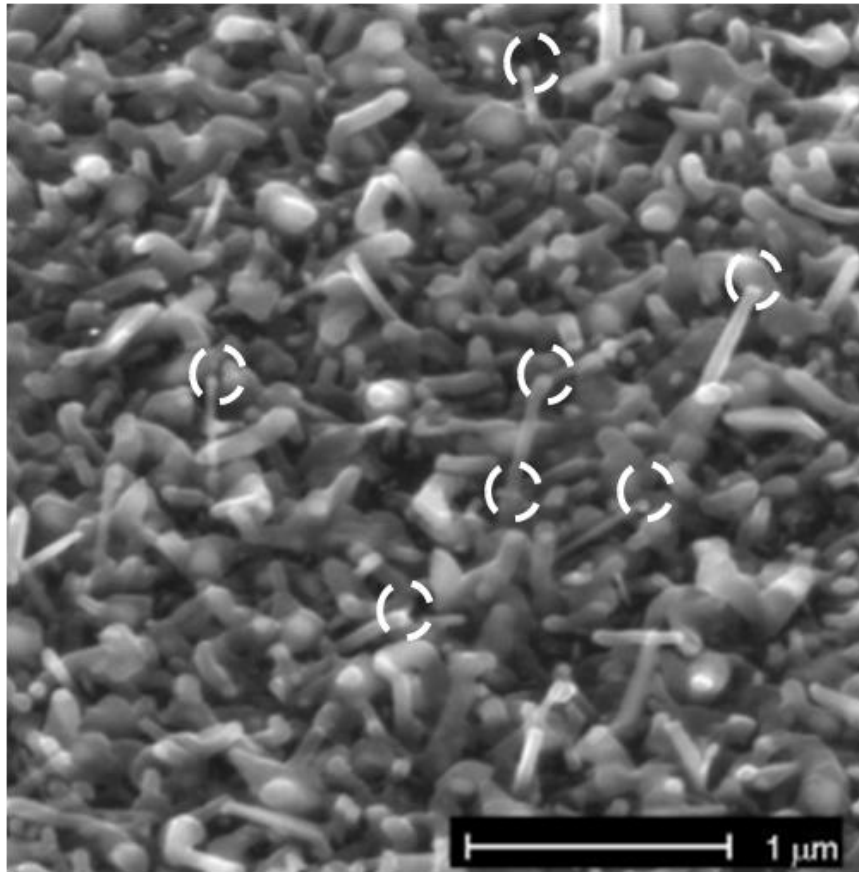


Figure 5. SEM image of Au alloy particles at the tips and at the bases of Au-catalyzed ZnO NWs grown by CVD technique

Comparison on Crystal Quality of ZnO Nanostructures

The stoichiometry of these ZnO specimens was characterized by XPS. As illustrated in Figure 6, the O 1s peak can be fitted by two Gaussian curves with the main peak (O_a) centered at 530.4 eV and the shoulder peak (O_b) centered at 532.2 eV [17]. The O_a peak is attributed to the Zn–O bonds, whereas the O_b peak is usually referred to chemisorbed or dissociated oxygen or OH species on the surface of ZnO e.g. $-\text{CO}_3$, adsorbed H_2O or adsorbed O_2 . The relative areas of the main O_a curve and the shoulder O_b curve of the ZnO specimens were calculated and shown in Table 1.

The catalyst-free ZnO NWs have relatively largest O_a percentage (Zn–O bonds) as compared to Au-catalyzed ZnO NWs and ZnO films. In other words, the catalyst-free ZnO NWs have fewer defects as it was mainly composed of Zn–O bonds. In contrary, the ZnO film has largest O_b percentage. This result was acceptable as the ZnO film could contain others components such as OH species and fragments of hydrocarbon due to incomplete decomposition of precursors [8].

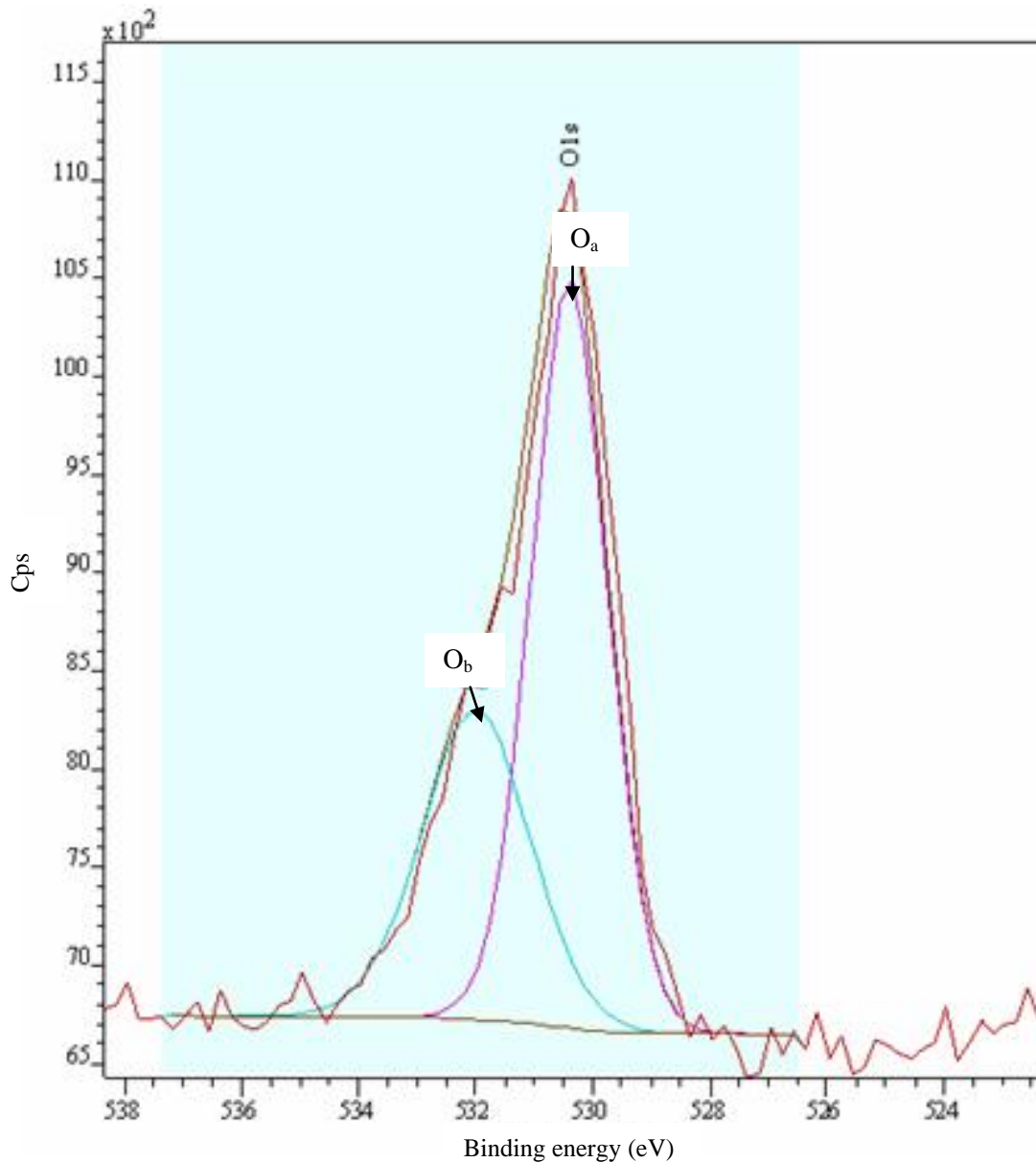


Figure 6. XPS spectrum of the O 1s peak of Au-catalyzed ZnO NWs, which could be fitted by two distributions, i.e O_a & O_b

Table 1: Relative Percentage of O_a and O_b Curves Area Calculated from XPS Results.

	% O _a (530.4 eV)	% O _b (532.2 eV)
Au-catalyzed ZnO NWs	63.20	36.80
ZnO film	52.01	47.99
Catalyst-free ZnO NWs	70.16	29.84

A dominant UV emission peak (377.3 nm) and a weak green emission peak (521.8 nm) were observed on these samples from room temperature PL measurement as shown in Figure 7. The UV emission peak of ZnO was referred to the near-band edge (NBE) emission of wide-band-gap ZnO whereas the green emission was related to crystal defects such as oxygen deficiency [18-19]. Thus, the UV/visible light intensity ratio of PL measurement is normally an indirect indication of the crystal quality of ZnO nanostructure.

The catalyst-free ZnO NWs exhibited the best crystal quality amongst these three ZnO nanostructures as it had the highest UV/visible light ratio, i.e. ~35. The UV/visible light intensity ratio of ZnO film was ~19, which was lower as compared to the catalyst-free ZnO NWs. This could be attributed to the presence of OH species or fragments of hydrocarbon in the film as a result of incomplete decomposition of precursors in this relatively low deposition temperature (145°C) [8]. The UV/visible light intensity ratio of Au-catalyzed ZnO NWs was the lowest ~15. This result indicates that the Au-catalyzed ZnO NWs have the poorest crystal quality. The cause of this observation needs further investigation although presence of trace Au in the ZnO NWs might deteriorate the crystal quality in addition to the contribution from the oxygen related defects.

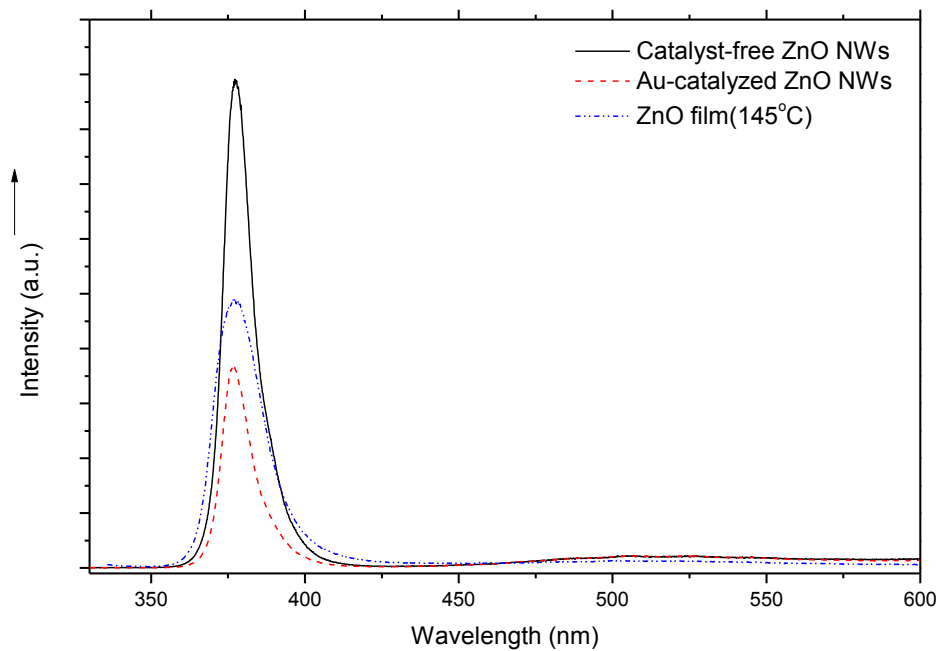


Figure 7. PL spectrum of catalyst-free ZnO NWs, Au-catalyzed ZnO NWs and ZnO film (145°C) measured at room temperature

Conclusions

Highly uniform and conductive ($4.131 \times 10^{-3} \Omega \cdot \text{cm}$) ZnO film could be produced by ALD at low temperature (145°C). The as-deposited ZnO film had a smooth surface (RMS roughness: 2.850 nm) and highly transmittance in the visible light region ($89.9 \pm 6.7\%$). Therefore, these ZnO films are suitable for transparent conducting oxide (TCO) applications. Vertically aligned ZnO NWs (catalyst-free) could be synthesized using highly (002) oriented ZnO seed film pre-deposited on silicon substrate. These NWs had the best crystal quality as compared to Au-catalyzed ZnO NWs and ZnO film as it had the largest percentage of Zn-O bonds in XPS analysis and highest UV/visible ratio in PL measurement. On the other hand, randomly grown Au-catalyzed ZnO NWs were synthesized on silicon substrates using CVD. The random alignment of NWs was attributed to the large lattice mismatch between ZnO and silicon wafer. A combined VLS-VS mechanism is proposed to describe the growth of Au-catalyzed ZnO NWs.

Acknowledgments

The financial support of AUN/SEED-Net and School of Materials and Mineral Resources Engineering, Universiti Sains Malaysia are gratefully acknowledged.

References

- [1] J.H. Lim, C.K. Kang, K.K. Kim, I.K. Park, D.K. Hwang, and S.J. Park, "UV electroluminescence emission from ZnO light-emitting diodes grown by high-temperature radio frequency sputtering," *Advanced Materials*, Vol. 18, No. 20, pp. 2720-2724, 2006.
- [2] H.T. Ng, J. Han, T. Yamada, P. Nguyen, Y.P. Chen, and M. Meyyappan, "Single crystal nanowire vertical surround-gate field-effect transistor," *Nano Letters*, Vol. 4, No. 7, pp. 1247-1252, 2004.
- [3] A.M. Peiro, P. Ravirajan, K. Govender, D.S. Boyle, P. O'Brien, D.C. Bradley, J. Nelson, and J.R. Durrant, "Hybrid polymer/metal oxide solar cells based on ZnO columnar structures," *Journal of Materials Chemistry*, Vol. 16, No. 21, pp. 2088-2096, 2006.
- [4] I.T. Tang, Y.C. Wang, W.C. Hwang, C.C. Hwang, N.C. Wu, M.P. Hwang, and Y.H. Wang, "Investigation of piezoelectric ZnO film deposited on diamond like carbon coated onto Si substrate under different sputtering conditions," *Journal of Crystal Growth*, Vol. 252, No. 1-3, pp. 190-198, 2003.
- [5] Y.K. Tseng, C.J. Huang, H.M. Cheng, I.N. Lin, K.S. Liu, and I.C. Chen, "Characterization and field emission properties of needle like zinc oxide nanowires grown vertically on conductive zinc oxide films," *Advanced Functional Materials* Vol. 13, No. 10, pp. 811-814, 2003.
- [6] Y. Sun, G.M. Fuge, N.A. Fox, D.J. Riley, and M.N.R. Ashfold, "Synthesis of aligned arrays of ultrathin ZnO nanotubes on a Si wafer coated with a thin ZnO film," *Advanced Materials*, Vol. 17, No. 20, pp. 2477-2481, 2005.
- [7] D.J. Park, D.C. Kim, J.Y. Lee, and H.K. Cho, "Synthesis and microstructural characterization of growth direction controlled ZnO nanorods using a buffer layer," *Nanotechnology*, Vol. 17, No. 20, pp. 5238-5243, 2006.
- [8] S.Y. Pung, K.L. Choy, X. Hou, and C. Shan, "Preferential growth of ZnO thin films by the atomic layer deposition technique," *Nanotechnology*, Vol. 19, p. 435609, 2008.
- [9] S. Ren, Y.F. Bai, J. Chen, S.Z. Deng, N.S. Xu, Q.B. Wu, and S. Yang, "Catalyst-free synthesis of ZnO nanowire arrays on zinc substrate by low temperature thermal oxidation," *Materials Letters*, Vol. 61, No. 3, pp. 666-670, 2007.
- [10] S. Oktik, *Progress In Crystal Growth And Characterization of Materials*, Vol. 17, p. 171, 1998.
- [11] J.H. Lee, B.W. Yeo, and B.O. Park, "Effects of the annealing treatment on electrical and optical properties of ZnO transparent conduction films by ultrasonic spraying pyrolysis," *Thin Solid Films*, Vol. 457, No. 2, pp. 333-337, 2004.
- [12] S.E. Demian, "Optical and electrical properties of transparent conducting ZnO films prepared by spray pyrolysis," *Journal of Materials Science: Materials in Electronics*, Vol. 5, No. 6, pp. 360-363, 1994.
- [13] S.Y. Pung, K.L. Choy, X.H. Hou, and C.X. Shan, "Growth morphology evolution of ZnO nanowires synthesized by chemical vapor deposition," *Crystal Growth: Theory, Mechanisms, and Morphology*, pp. 155-211, 2012.
- [14] S.Y. Pung, K.L. Choy, E.A. Vinogradov, N.N. Novikova, and V.A. Yakovlev, "Structural and Infrared analysis of ZnO film and nanowires," *Journal of Crystal Growth*, Vol. 312, No. 15, pp. 2220-2225, 2010.

- [15] W. Lu, and C.M. Lieber, "Semiconductor nanowires," *Journal of Physics D: Applied Physics*, Vol. 39, No. 21, pp. R387-R406, 2006.
- [16] S.Y. Pung, K.L. Choy, and X.H. Hou, "Tip-growth mode and base-growth mode of Au-catalyzed ZnO nanowires using chemical vapour deposition technique," *Journal of Crystal Growth*, Vol. 312, No. 14, pp. 2049-2055, 2010.
- [17] S. Jeon, S. Bang, S. Lee, S. Kwon, W. Jeong, H. Jeon, H.J. Chang, and H.H. Park, "Structural and electrical properties of ZnO thin films deposited by atomic layer deposition at low temperatures," *Journal of the Electrochemical Society*, Vol. 155, No. 10, pp. H738-H743, 2008.
- [18] S. Monticone, R. Tufeu, and A.V. Kanaev, "Complex nature of the UV and visible fluorescence of colloidal ZnO nanoparticles," *Journal of Physical Chemistry B*, Vol. 102, No. 16, pp. 2854-2862, 1998.
- [19] J.J. Wu, and S.C. Liu, "Low-temperature growth of well-aligned ZnO nanorods by chemical vapor deposition," *Advanced Materials*, Vol. 14, No. 3, pp. 215-218, 2002.